Article

Chinese Science Bulletin

Inorganic Chemistry

October 2011 Vol.56 No.30: 3199–3203
doi: 10.1007/s11434-011-4653-2

Synthesis and magnetic properties of Fe_3O_4/helical carbon nanofiber nanocomposites from the catalytic pyrolysis of ferrocene

ZHANG JunHao[1,2*], WANG JiaoLong[2], WANG HongLiang[2], JIA Liang[2], QU ZhaoKun[2] & QIAN YiTai[1]

[1] *School of Chemistry and Chemical Engineering, Shandong University, Jinan 250100, China;*
[2] *School of Biological and Chemical Engineering, Jiangsu University of Science and Technology, Zhenjiang 212018, China*

Received April 4, 2011; accepted May 5, 2011

High purity Fe_3O_4/helical carbon nanofiber composites were obtained on a large scale by the catalytic pyrolysis of ferrocene in the presence of tin powder at 500°C over 12 h. The sizes of Fe_3O_4 nanoparticles are 35–65 nm in size, and the diameters of the helical carbon nanofibers range from 40–70 nm. The shapes and compositions of the nanocomposites are simply controlled by adjusting the reaction temperatures. On the basis of the obtained experimental results the formation of the helical Fe_3O_4/carbon nanofiber composites was investigated and discussed. The magnetic hysteresis loop of the products shows ferromagnetic behavior with saturation magnetization (M_s), remanent magnetization (M_r) and coercivity (H_c) values of *ca*. 29.8 emu/g, 9.6 emu/g and 306.6 Oe, respectively.

helical carbon nanofiber, catalytic pyrolysis, scanning and transmission electron microscopy, magnetic property

Citation: Zhang J H, Wang J L, Wang H L, et al. Synthesis and magnetic properties of Fe_3O_4/helical carbon nanofiber nanocomposites from the catalytic pyrolysis of ferrocene. Chinese Sci Bull, 2011, 56: 3199–3203, doi: 10.1007/s11434-011-4653-2

Carbon nanotubes were first observed in 1991 [1] and this discovery stimulated intense interest in the synthesis and physical properties of carbon nanotubes because of their potential applications. Apart from cylindrical carbon nanotubes, differently shaped carbon nanomaterials have also been observed. Much attention has been paid to the study of coiled carbon nanofibers and carbon nanotubes because of their novel coiled morphologies, which gives interesting physical properties and diverse applications [2–9]. They can be used as electromagnetic wave absorbers and filters, microdevices, micro-sensors, hydrogen storage materials, electrode materials, catalyst supports, elastic materials, strengthening fibers in composite materials, mechanical components and field emission materials [10–15]. Their elastic and mechanical properties are among their most important properties. Luo et al. [16] reported the synthesis of helically coiled carbon nanotubes by reducing the amount of ethyl ether and using Zn as a catalyst at 700°C. Yang et al. [17] reported that three-dimensional spring-like carbon nanocoils were obtained in high purity and high yield by the catalytic pyrolysis of acetylene at 750–790°C using an Fe-based catalyst. Bajpai et al. [18] demonstrated that large scale aligned helical carbon nanotube arrays perpendicular to the substrate surface can be prepared by the co-pyrolysis of $Fe(CO)_5$ and pyridine onto pristine quartz glass plates in a tube furnace at 900–1100°C under a mixted flow of Ar and H_2. Carbon microcoils, a type of novel carbon material with a 3D double-helix/spiral structure similar to DNA were obtained by the Ni-catalyzed pyrolysis of acetylene at 750°C [19]. In general, they were prepared by the high-temperature (>600°C) catalytic decomposition of an organic vapour of acetylene or pyridine with transition-metal catalysts such as Ni and Fe. In this study, we describe the novel synthesis of Fe_3O_4/helical carbon nanofiber nanocomposites by the

*Corresponding author (email: jhzhang6@mail.ustc.edu.cn)

pyrolysis of ferrocene in the presence of tin at 500°C.

1 Experimental

All the reagents are commercially available and were used without further purification. In a typical experiment, ferrocene (0.50 g) and Sn powder (0.50 g) were added to an autoclave with 20 mL capacity. The autoclave was tightly sealed and heated in an electric stove. The stove temperature was raised to 500°C at a heating ramp rate of 10 °C min^{-1} and maintained at 500°C for 12 h upon which it was allowed to cool to room temperature naturally. We found that the final products in the autoclave included many dark precipitates and some residual gases. The dark products on the wall were collected and washed with absolute ethanol and distilled water. The final products were dried in a vacuum at 50°C over 6 h.

The X-ray diffraction (XRD) patterns were obtained on a Rigaku (Japan) D/max-γA X-ray diffractometer with Cu Kα radiation ($\lambda = 1.54178$ Å). Raman spectra were obtained at ambient temperature on a Spex 1403 Raman spectrometer (Ar ion laser, 514.5 nm). FESEM (JEOL JSM-6700F) was used to observe the morphologies of products. The TEM images and HRTEM image were obtained on a JEOL-2010 transmission electron microscope. The magnetic properties (M-H curve) were measured at room temperature on an MPMS XL magnetometer made by Quantum Design Corporation.

2 Results and discussion

Figure 1(a) shows the powder XRD pattern of the products and these were prepared at 500°C over 12 h, and washed several times using distilled water and ethanol. According to the diffraction peaks in the figure, the main phases in the products can be indexed as face-centered cubic (fcc) Fe_3O_4 (JCPDS Card no. 85-1436) and hexagonal graphite (JCPDFS Card no. 48-1487). The representative Raman spectrum (Figure 1(b)) of the products shows a typical carbon nanofiber feature. In detail, two strong peaks are present at 1594 and 1335 cm^{-1}, which correspond to typical Raman peaks of graphitized carbon nanostructures. The peak at 1594 cm^{-1} is attributed to the Raman-active $E2g$ in-plane vibration mode and is related to the vibration of sp^2-bonded carbon atoms in a two-dimensional hexagonal lattice. The peak at 1335 cm^{-1} is associated with the vibrations of carbon atoms with dangling bonds at the plane terminations of disordered graphite. The intensity of the D-band peak is strong, which originates from the in-plane defects of the products preventing the layer from extending.

The morphology of the products was investigated using FESEM and TEM observation, and these indicated that the products are composed of helical structures and the yield was more than 95%. Figure 2(a) shows a typical FESEM image of the high yield products. From Figure 2(b), the products are helical structures with diameters of about 40–70 nm and lengths of several micrometers. The structures were further characterized by TEM. Figure 2(c) shows a TEM image of the products, which agrees with the above FESEM images. A notable result is that the average diameters of the carbon nanofibers and the Fe_3O_4 nanoparticles are all about 35–65 nm, which indicates that the size of the Fe_3O_4 nanoparticles determines the diameter of the carbon nanofibers. In Figure 2(d), the lattice plane spacing calculated from the HRTEM image is *ca*. 0.295 nm, which corresponds to the *hkl* (220) of a typical fcc Fe_3O_4 structure.

To understand the possible formation processes of Fe_3O_4/helical carbon nanofiber composites, a series of relevant experiments were carried out by altering the experimental parameters. It is obvious that the reaction temperature plays a critical role in the formation of Fe_3O_4/helical carbon nanofiber composites. At a reaction temperature of 500°C the products are Fe_3O_4/helical carbon nanofiber composites. Figure 3 shows TEM images and XRD patterns of the products obtained at 600 and 700°C. Figure 3(a) shows that the main products are flake-like structures for a reaction temperature of 600°C. Figure 3(b) indicates that the products consist of two parts: an outer shell and an inner core while

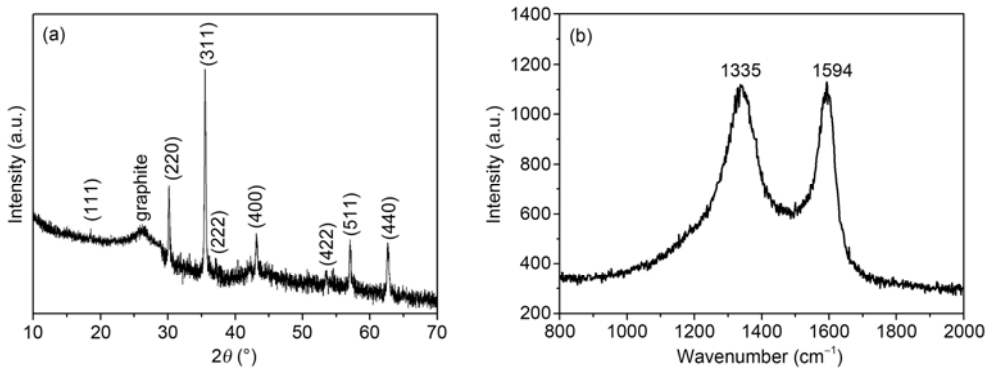

Figure 1 (a) XRD pattern of the products obtained at 500°C over 12 h; (b) Raman spectrum of the products obtained at 500°C over 12 h.

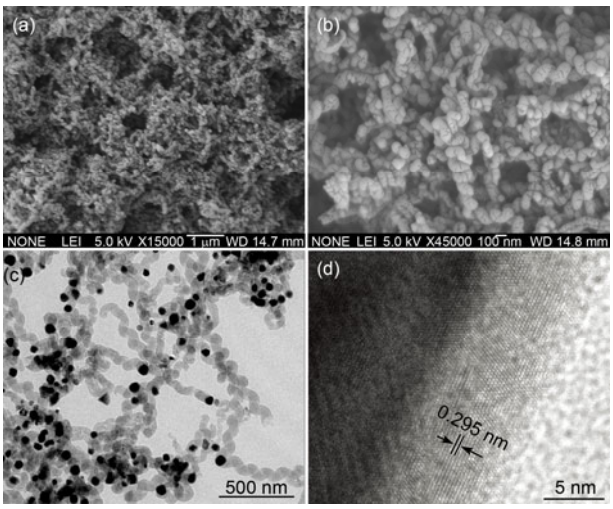

Figure 2 (a) Low magnification FESEM image of Fe_3O_4/helical carbon nanofiber composites obtained at 500°C over 12 h; (b) high magnification FESEM image of Fe_3O_4/helical carbon nanofiber composites obtained over 500°C over 12 h; (c) low magnification TEM image of Fe_3O_4/helical carbon nanofiber composites obtained at 500°C over 12 h; (d) HRTEM image of Fe_3O_4/helical carbon nanofiber composites obtained at 500°C over 12 h.

the shell thickness of the large flakes is about 6 nm. XRD (Figure 3(e)) confirms that the products are carbon and Fe_3O_4, which agrees with the TEM images. By increasing the reaction temperature to 700°C, carbon coated nanoparticles were obtained, as shown in Figure 3(c). Figure 3(d) indicates that the size of nanoparticles is about 48 nm and the thickness of shells is about 4 nm. TEM images and XRD (Figure 3(f)) indicate that the products are carbon coated Fe nanoparticles.

In this system, we found that the reaction temperature plays a crucial role in the controlled synthesis of the different composites. Although the detailed mechanism is not fully understood at present it is likely that Fe atoms are released by the decomposition of ferrocene (decomposition temperature: 400°C [20]) and Fe nanoparticles form with an increase in temperature. At 500°C Fe nanoparticles react with O_2 in a sealed reaction system to form Fe_3O_4 nanoparticles but the catalytic decomposition of C_5H_5 to carbon is slow because of the lower temperature, and this results in that the formed carbon having adequate time to grow vertically in the (002) crystal plane direction, leading to the formation of Fe_3O_4/helical carbon nanofiber composites. However, a question arises about why helical carbon nanofibers are obtained. To create carbon helical structures, transition metal tin compounds have been used as catalysts [21]. At a reaction temperature of 600°C, the lower amount of O_2 causes the nucleation rate of the Fe_3O_4 particles to slow but the catalytic decomposition of C_5H_5 to carbon is fast because of the high temperature. Compared with fast nucleation and aggregation growth the slower aggregation growth of Fe_3O_4 allows for an adequate rotation of the crystals to find a low energy configuration interface and to form perfectly oriented aggregates. Similar to the gold or silver

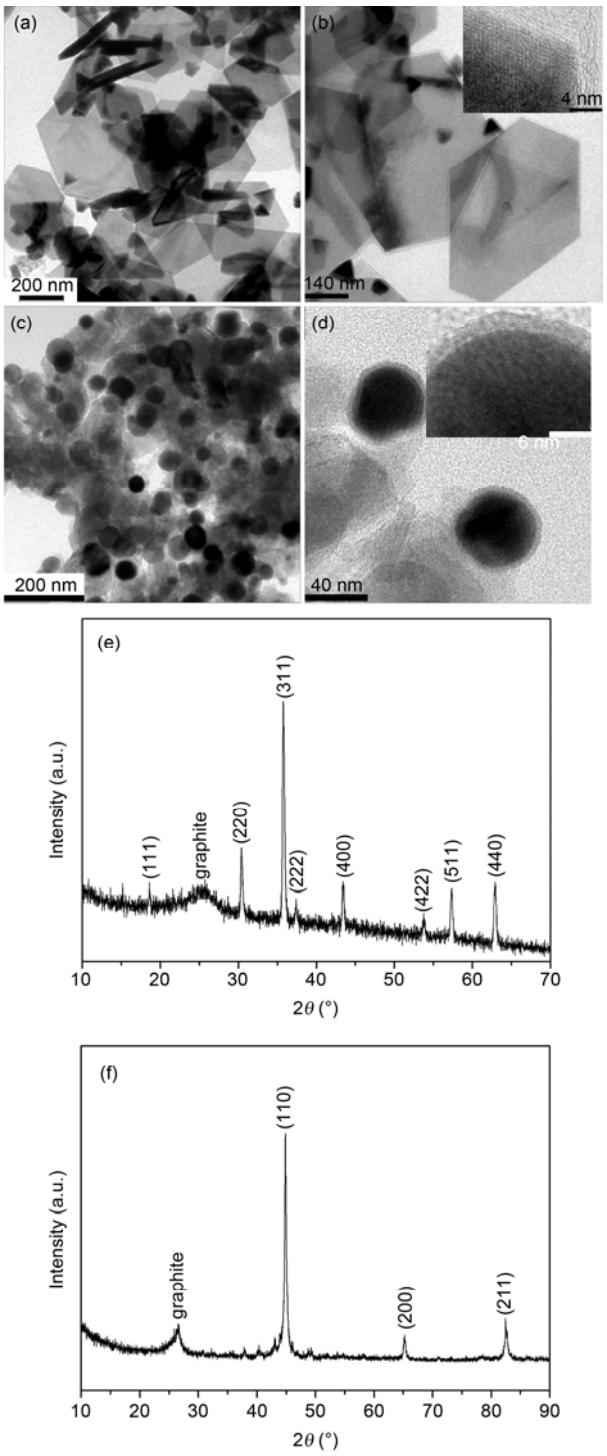

Figure 3 (a) and (b) different magnification TEM images of the products obtained at 600°C over 12 h, and the HRTEM image (inset) in (b); (c) and (d) different magnification TEM images of products obtained at 700°C over 12 h and the HRTEM image (inset) in (d); (e) XRD pattern of the products obtained at 600°C over 12 h; (f) XRD pattern of the products obtained at 700°C over 12 h.

triangular fcc crystals [22,23] the (111) plane of Fe_3O_4 may also possess the lowest surface energy. Therefore, flake-like Fe_3O_4 might be formed with the (111) plane as a basal plane. At the same time, some carbon feed stock would cover the

flake-like Fe_3O_4 particles to form flake-like Fe_3O_4@C composites [24]. At a reaction temperature of 700°C the as-formed iron nanoparticles are quickly wrapped by a small number of carbon atoms (forming a thin carbon lamella) to reduce their surface energy and form Fe nanoparticles encapsulated within thin carbon capsules. These thin carbon lamella restrict the growth of the formed Fe nanoparticles. As carbon atoms are released in these experiments the continued addition (or diffusion) of carbon atoms finally leads to the formation of carbon coated Fe nanoparticles, as shown in Figure 3(c).

Magnetization measurements were carried out to examine the magnetic properties at room temperature with an applied field from −5000 to 5000 Oe, as shown in Figure 4. The magnetic hysteresis loop of the products at 500°C shows ferromagnetic behavior with saturation magnetization (M_s), remanent magnetization (M_r), and coercivity (H_c) values of *ca*. 29.8 emu/g, 9.6 emu/g and 306.6 Oe, respectively. From these results, the saturation magnetization value of the products is lower than that of bulk Fe_3O_4 (85–100 eum/g). The decrease in the M_s found in this work might be caused by two factors. On the one hand, the wide existence of carbon nanofibers is likely. The results of the burring experiments indicate that the calculated Fe_3O_4 to Fe_3O_4/helical carbon nanofibers mass ratio of the products is about 0.384. On the other hand, the presence of a detrimental surface/crystal-structure is also related to the demagnetization effects. However, the coercivity value is higher than that of sub-microspheres (124.7 Oe) and Fe_3O_4 nanopartiicles (274 Oe) [25,26]. These research results indicate that size and morphology may be influencing factors because the coercivity is sensitive to many structural parameters such as the internal stress, the orientation, defects and shapes.

3 Conclusions

In summary, Fe_3O_4/helical carbon nanofiber composites were synthesized at 500°C for 12 h in a sealed reaction system. The yield of Fe_3O_4/helical carbon nanofiber composites was more than 95%. By controlling the reaction temperature, flake-like Fe_3O_4 nanocomposites and carbon coated Fe nanoparticles were obtained at 600 and 700°C over 12 h. The growth mechanism of the Fe_3O_4/helical carbon nanofibers composites is discussed. The Fe_3O_4/helical carbon nanofibers composites show that the saturation magnetization (29.8 emu/g) and coercivity (306.6 Oe) are different from those of bulk Fe_3O_4, sub-microspheres and Fe_3O_4 nanoparticles, which can be attributed to the different carbon content, size and morphology of the products.

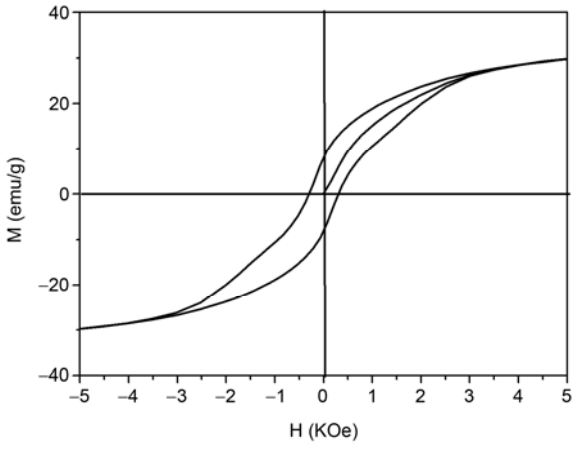

Figure 4 Magnetic hysteresis loop of the Fe_3O_4/helical carbon nanofiber composites obtained at 500°C over 12 h.

This work was supported by the National Basic Research Program of China (2011CB935901) and the Start Fund for Advanced Professional of Jiangsu University of Science and Technology (35060810).

1 Iijima S. Helical microtubules of graphitic carbon. Nature, 1991, 354: 56–58
2 Liu D Y, Luo Q M, Wang H X, et al. Direct synthesis of micro-coiled carbon fibers on graphite substrate using co-electrodeposition of nickel and sulfur as catalysts. Mater Design, 2009, 30: 649–652
3 Zheng T L, Wang Y H, Zheng K Y, et al. Electromagnetism and absorptivity of the modified micro-coiled chiral carbon fibers. Chinese J Aeronaut, 2007, 20: 559–563
4 Qin Y H, Zhang Y H, Sun X. Synthesis of helical and straight carbon nanofibers by chemical vapor deposition using alkali chloride catalysts. Microchim Acta, 2009, 164: 425–430
5 Yu L Y, Sui L N, Qin Y, et al. Low-temperature synthesis of carbon nanofibers by decomposition of acetylene with a catalyst derived from cupric nitrate. Chem Eng J, 2008, 144: 514–517
6 Kong Q H, Zhang J H. Synthesis of straight and helical carbon nanotubes from catalytic pyrolysis of polyethylene. Polym Degrad Stabil, 2007, 92: 2005–2010
7 Nitze F, Abou-Hamad E, Wagberg T. Carbon nanotubes and helical carbon nanofibers grown by chemical vapour deposition on C-60 fullerene supported Pd naniparticles. Carbon, 2011, 49: 1101–1107
8 Tang N J, Wen J F, Zhang Y, et al. Helical carbon nanotubes: Catalytic particle size-dependent growth and magnetic properties. ACS Nano, 2010, 4: 241–250
9 Tang N J, Zhong W, Au C T, et al. Large-scale synthesis, annealing, purification, and magnetic properties of crystalline helical carbon nanotubes with symmetrical structures. Adv Funct Mater, 2007, 17: 1542–1550
10 Motojima S, Chen X Q. Preparation and characterization of carbon microcoils. Bull Chem Soc Japan, 2007, 80: 449–455
11 Yang S M, Chen X Q, Motojima S. Coiling-chirality changes in carbon microcoils obtained by catalyzed pyrolysis of acetylene and its mechanism. Appl Phys Lett, 2002, 81: 3567–3569
12 Singh R K, Raghubanshi H, Pandey S K, et al. Effect of admixing different cabon structural variants on the decomposition and hydrogen sorption kinetics of magnesium hydride. Int J Hydrog Energy, 2010, 35: 4131–4137
13 Zhang L, Li F. Helical nanocoiled and microcoiled carbon fibers as effective catalyst supports for electrooxidation of methanol. Electrochem Acta, 2010, 55: 6695–6702
14 Ren X, Zhang H, Cui Z L. Acetylene decomposition to helical carbon nanofibers over supported copper catalysts. Mater Res Bull, 2007, 42: 2202–2210
15 Motojima S, Chen X Q. Preparation and characterization of carbon microcoils. Bull Chem Soc Japan, 2007, 80: 449–455
16 Luo T, Liu J W, Chen L Y, et al. Synthesis of helically coiled carbon nanotubes by reducing ethyl ether with metallic zinc. Carbon, 2005, 43: 755–759
17 Yang S M, Chen X Q, Motojima S, et al. Morphology and micro-

structure of spring-like carbon micro-coils/nano-coils prepared by catalytic pyrolysis of acetylene using Fe-containing alloy catalysts. Carbon, 2005, 43: 827–834
18 Bajpai V, Dai L M, Ohashi T. Large-scale synthesis of perpendicularly aligned helical carbon nanotubes. J Am Chem Soc, 2004, 126: 5070–5071
19 Chen X Q, Yang S M, Motojima S. Morphology and growth models of circular and flat carbon coils obtained by the catalytic pyrolysis of acetylene. Mater Lett, 2002, 57: 48–54
20 Bernhauer M, Braun M, Hüttinger K J. Kinetics of mesophase formation in a stirred tank reactor and properties of the products—V. Catalysis by ferrocene. Carbon, 1994, 32: 1073–1085
21 Wang W, Yang K Q, Gaillard J, et al. Rational synthesis of helically coiled nanowires and nanotubes through the use of tin and indium catalysts. Adv Mater, 2008, 20: 179–182
22 Sun Y G, Mayers B, Xia Y N. Transformation of silver nanospheres into nanobelts and triangular nanoplates through a thermal process. Nano Lett, 2003, 3: 675–679
23 Umar A A, Oyama M. Formation of gold nanoplates on indium tin oxide surface: Two-dimensional crystal growth from gold nanoseed particles in the presence of poly(vinylpyrrolidone). Cryst Growth Des, 2006, 6: 818–821
24 Zhang J H, Du J, Qian Y T, et al. Shape-controlled synthesis and their magnetic properties of hexapod-like, flake-like and chain-like carbon-encapsulated Fe_3O_4 core/shell composites. Mater Sci Eng B, 2010, 170: 51–57
25 Zhang J H, Kong Q H, Lu W L, et al. Synthesis, characterization and magnetic properties of near monodisperse Fe_3O_4 sub-microspheres. Chinese Sci Bull, 2009, 54: 2434–2439
26 Zhang J H, Du J, Ma D K, et al. One-dimensional chain Fe_3O_4 nanoparticles encapsulated in worm-shaped carbon shell. Solid State Commun, 2007, 144: 168–173